Excess electron states in reduced bulk anatase TiO_2: Comparison of standard GGA, $GGA+U$, and hybrid DFT calculations

Emanuele Finazzi, Cristiana Di Valentin, Gianfranco Pacchioni, , and Annabella Selloni

Citation: J. Chem. Phys. **129**, 154113 (2008); doi: 10.1063/1.2996362
View online: http://dx.doi.org/10.1063/1.2996362
View Table of Contents: http://aip.scitation.org/toc/jcp/129/15
Published by the American Institute of Physics

Excess electron states in reduced bulk anatase TiO_2: Comparison of standard GGA, GGA+*U*, and hybrid DFT calculations

Emanuele Finazzi,[1] Cristiana Di Valentin,[1] Gianfranco Pacchioni,[1,a)] and Annabella Selloni[2]
[1]*Dipartimento di Scienza dei Materiali, Università di Milano-Bicocca, Via R. Cozzi 53, 20125 Milano, Italy*
[2]*Department of Chemistry, Princeton University, Princeton, New Jersey 08540, USA*

(Received 23 July 2008; accepted 15 September 2008; published online 20 October 2008)

The removal of lattice O atoms, as well as the addition of interstitial H atoms, in TiO_2 is known to cause the reduction in the material and the formation of "Ti^{3+}" ions. By means of electronic structure calculations we have studied the nature of such oxygen vacancy and hydrogen impurity states in the bulk of the anatase polymorph of TiO_2. The spin polarized nature of these centers, the localized or delocalized character of the extra electrons, the presence of defect-induced states in the gap, and the polaronic distortion around the defect have been investigated with different theoretical methods: standard density functional theory (DFT) in the generalized-gradient approximation (GGA), GGA+*U* methods as a function of the *U* parameter, and two hybrid functionals with different admixtures of Hartree–Fock exchange. The results are found to be strongly dependent on the method used. Only GGA+*U* or hybrid functionals are able to reproduce the presence of states at about 1 eV below the conduction band, which are experimentally observed in reduced titania. The corresponding electronic states are localized on Ti 3*d* levels, but partly delocalized solutions are very close in energy. These findings show the limited predictive power of these theoretical methods to describe the electronic structure of reduced titania in the absence of accurate experimental data. © *2008 American Institute of Physics*. [DOI: 10.1063/1.2996362]

I. INTRODUCTION

The description of defects in wide band gap or insulating oxides is an important challenge for modern electronic structure theory methods.[1–4] Electrons or holes associated to a given defect (a vacancy, an interstitial or impurity atom, a morphological defect, etc.) can be localized or delocalized depending on the nature of the oxide, the character of the electronic states, and the degree of local polaronic distortion following the formation of the defect. A typical signature of the presence of defects in the bulk or at the surface of the material is the appearance of new states in the gap. Depending on the energy and character of these states, the properties of the material (color, optical properties, magnetic properties, conductivity, reactivity, etc.) may change substantially and lead to completely different behaviors.[5,6] Thus, the correct description of the energy of the defect states in the gap and of the localized or delocalized nature of the associated electrons and holes is of crucial importance to properly account for the properties of the oxide.

In the past decade many examples have been reported that illustrate the difficulty of density functional theory (DFT) methods to describe the properties of defects in insulators, as discussed in a recent review.[7] A classical case is that of a neutral Al impurity in quartz-SiO_2 (Refs. 8–15) where standard DFT methods in the generalized-gradient approximation (GGA) produce a hole delocalized over four O atoms around the Al impurity,[16,17] at variance with the experimental evidence which shows full localization on a single oxygen. This is due to the self-interaction[18,19] in DFT and the consequent tendency to delocalize unpaired electrons in order to reduce the Coulomb repulsion. This problem is well known for complex systems like narrow band oxides,[20] and has been early recognized for molecular systems.[21] It can be eliminated or reduced by using the many-body GW approximation[22] or using more "pragmatic" approaches, i.e., either using hybrid functionals, where the "exact" Hartree-Fock (HF) exchange is partly mixed-in with the DFT exchange, or by means of the so-called DFT+*U* approaches.[23] This approach corrects some of the inadequacies connected to the DFT treatment of localized states, but suffers from the dependence of the results on the value of *U*, *de facto* an empirical parameter (*U* can be in principle determined in a self-consistent and basis-set independent way,[24] but the calculations can be cumbersome and the results are not necessarily better than using an empirical *U*). Also hybrid functionals, however, suffer from the same problem: the amount of HF exchange is a tunable parameter.

The situation is even more complex in the case of wide-gap semiconductors like titanium dioxide. TiO_2 has a band gap of 3 eV (rutile)[25,26] or 3.2 eV (anatase).[27] The primary structural difference between the two phases is that anatase is 9% less dense than rutile, and has larger Ti-Ti distances, a more pronounced localization of the Ti 3*d* states and a narrower 3*d* band.[28–30] Titania is usually employed in a reduced form where the level of reduction results in a more or less pronounced blue color. The nature of reduced TiO_2 has been the subject of a large number of experimental and theoretical studies.[31,32] Most of these studies are performed on the sur-

a)Electronic mail: gianfranco.pacchioni@unimib.it.

face of rutile TiO_2 (see Ref. 7 and 33 and references therein). Particularly relevant in this context is the DFT+U studies of Morgan and Watson and Calzado *et al.*[34] on rutile (110) surface where the dependence of the results on the U value has been carefully examined. Only few theoretical studies have considered the nature of an isolated O vacancy in bulk anatase,[35–37] and none has been performed with hybrid functionals (three studies performed at the B3LYP level were reported for the rutile surface[3,38,39]).

The main results emerging from experimental studies of reduced TiO_2 can be summarized as follows and are common to both rutile and anatase. Removal of lattice oxygen atoms leads to new species identified as "Ti^{3+} ions";[40,41] these can be lattice ions in pseudo-octahedral coordination or interstitials in distorted octahedral environment. The presence of the Ti^{3+} ions is accompanied by some spectroscopic signatures: (1) the appearance of absorption bands in the visible region which are responsible for the change in color and which have been assigned to *d-d* transitions;[42] (2) the occurrence of a new state in the gap at about 0.8–0.9 eV below the conduction band attributed to the reduced Ti^{3+} ions;[43,44] (3) the presence of more than one EPR signal associated to various kinds of paramagnetic Ti^{3+} ions in the lattice;[42–49] (4) a shift in the core level binding energies of the reduced Ti atoms.[50] While the details on the local environment and the relative abundance of the defect centers depend on various parameters (surface area, anatase versus rutile, presence of hydroxyl groups, sample preparation, etc.),[51] features (1)–(4) are the most important signatures characterizing a reduced titania sample. In order to provide reliable information about the properties of reduced titania, any electronic structure method should thus be able to reproduce these features, and in particular the paramagnetic nature of the centers and the presence of a state in the gap.

Many of the available theoretical studies on reduced titania are based on standard DFT calculations.[52–54] In these studies usually the band gap, typically 2–2.5 eV, is too small compared to experiment; moreover, no defect state is present in the gap and spin properties are ignored. While this may be enough to obtain a qualitative picture, it is certainly not sufficient to describe problems which involve electron excitation and photoexcitation, near-conduction band states, radical reactions, electron localization, etc. For these problems a more accurate description is needed and examples on the specific case of titania have been reported.[55] As we mentioned above, however, it is not clear which theoretical method can provide the best answers to these questions.

In this work we report a careful comparison of various DFT methods, including pure GGA [exchange-correlation functional by Perdew, Burke and Ernzerhof (PBE)], GGA+U (with 2 eV$\leq U \leq$4 eV), and hybrid functionals (B3LYP, with 20% HF exchange and H&HLYP, with 50% HF exchange), in the description of an oxygen vacancy and a hydrogen impurity in the bulk of anatase TiO_2. The oxygen removal has basically the same effect as the addition of an H atom to stoichiometric TiO_2: both processes lead to the presence of extra electrons, which formally reduce Ti, $Ti^{4+}+e^- \rightarrow Ti^{3+}$. Despite the abundance of experimental data, some questions related to the electronic structure of these defects are still without answer. Here we consider only the formation of reduced Ti^{3+} ions in octahedral lattice positions, not that of interstitial Ti ions. The former (lattice ions) are supposed to form in the early phases of reduction, by mild thermal treatment or by doping with heteroatoms (e.g., F);[56] the latter (interstitials) are most probably formed under more severe conditions (high temperature annealing, surface sputtering, etc.).[57–61] The aim of this study is to analyze the response of various methods in the presence of the same defect. In particular we shall focus on the spin localization and spin distribution, the position of the defect states in the gap, and the local distortion around the defect.

II. COMPUTATIONAL DETAILS

The calculations, which include spin polarization, have been performed using the generalized gradient approximation (GGA) with the PBE (Ref. 62) functional, the GGA+U method[23,63,64] (with the same PBE functional), and the hybrid B3LYP (Refs. 65 and 66) and H&HLYP functionals. For the case of an oxygen vacancy, with two extra electrons, a triplet state has been considered; for the case of an H impurity the spin state is a doublet. For the PBE and GGA+U calculations a plane wave basis set was used. The cutoffs for the smooth part of the wave function and the augmented density were 25 and 200 Ry, respectively, as implemented in the Quantum ESPRESSO code.[67] In GGA+U a set of atomic-like orbitals is treated with a new Hamiltonian,[23,63] which depends on the difference $U=U'-J$,[24] where U' is a parameter, which describes the energy increase for an extra electron on a particular site, and J is a second parameter, which represents the screened exchange energy. Various values of U=2, 3, and 4 eV have been used for the Ti 3*d* orbitals.

In the hybrid functional calculations the Kohn–Sham orbitals are expanded in Gaussian-type orbitals (GTO), as implemented in the CRYSTAL06 code[68] [the all-electron basis sets are Ti 86 411(d41) (Ref. 69) and O 8411(d1) (Ref. 70)]. For an improved description of the Ti^{3+} species we have added a more diffuse d function with α exponent=0.13. The percentage of exact HF exchange is 20% in the B3LYP functional and 50% in the H&HLYP functional (*H&H*=half&half).[71]

We considered a nearly cubic $2\sqrt{2}\times 2\sqrt{2}\times 1$ supercell (96 atoms) to model doped anatase. The optimized bulk lattice parameters were taken from previous PBE (a=3.786 Å and c=9.737 Å) (Ref. 72) and B3LYP (a=3.776 Å and c=9.866 Å) calculations.[73] Full geometry optimization was performed until the largest component of the ionic forces was less than 1×10^{-4} a.u. (PBE and GGA+U) or 5×10^{-4} a.u. (hybrid functionals). The k-space sampling was restricted to a special k-point (0.25, 0.25, 0.2749), in the irreducible part of the Brillouin zone, for the plane wave self-consistent field calculations and to the Γ-point for the CRYSTAL calculations. The CRYSTAL densities of states (DOS) have been obtained with a 36 k-points mesh.

TABLE I. Selected distances (in Å) in stoichiometric and reduced bulk anatase TiO_2.

		Stoichiometric TiO_2			Reduced TiO_2		
Method	U (eV)	d(Ti–Ti)	d(Ti–O_{eq})	d(Ti–O_{ax})	d(Ti_1–Ti_2)	d(Ti_4–O_2)	d(Ti_3–O_1)
PBE	···	3.786	1.941	2.006	4.279	2.351	2.351
GGA+U	2	3.786	1.941	2.006	4.064	2.204	2.028
GGA+U [a]	3	3.786	1.941	2.006	4.053	2.237	2.057
GGA+U [b]	3	3.786	1.941	2.006	4.061	2.229	2.033
GGA+U	4	3.786	1.941	2.006	4.041	2.258	2.056
B3LYP[a]	···	3.777	1.945	2.014	4.145	2.454	2.123
B3LYP[b]	···	3.777	1.945	2.014	4.180	3.064	1.998
H&HLYP	···	3.777	1.945	2.001	4.196	2.870	2.114
Experimental (Ref. 74)	···	···	1.936	1.981	···	···	···

[a]Localized solution, see Table II.
[b]Semilocalized solution, see Table II.

III. RESULTS AND DISCUSSION

A. Oxygen vacancy in bulk anatase

The tested theoretical methods yield structural parameters for stoichiometric bulk anatase, which are all very similar and in substantial agreement with the experimental data,[74] as reported also in a recent theoretical study on this topic.[75] No difference is found in Ti–O distances between PBE and GGA+U methods, and also the differences with respect to hybrid functionals are minor, often smaller than 0.01 Å, Table I. On the basis of these results, one can conclude that the structure of nondefective anatase is properly described no matter which DFT method is used. However things change significantly when one considers reduced TiO_2.

Upon removal of a lattice oxygen in bulk anatase, the atoms around the defect undergo displacements that strongly depend on the method used. In Fig. 1 we show schematically the geometry of this defect center as obtained at PBE, GGA+U (U=3 eV) and B3LYP levels of theory. For a better identification of the atomic displacements, we also refer to Table I where some relevant interatomic distances are reported.

With respect to the nondefective oxide, the distance between two Ti ions adjacent to the vacancy increases considerably and is always longer in PBE than in GGA+U or hybrid calculations, Table I. Moreover, the O_1 and O_2 atoms move toward the vacant site V_O in Fig. 1 so that their distance from the adjacent Ti ions also increases, but to a different extent, depending on the method used. The displacement in PBE is symmetric while it is asymmetric in all GGA+U and in hybrid calculations, Table I. With the hybrid methods the asymmetry of the distortion can be very pronounced, with the Ti_4–O_2 distance more than 1 Å longer than the Ti_3–O_1 one, Table I. Thus, a first conclusion is that the level of local relaxation around the defect is remarkably different depending on the method used. While all methods provide a very similar structure of the stoichiometric oxide, this is no longer the case for the defective one.

In order to rationalize the above differences it is important to carefully analyze the electronic structure of the system. We have focused our attention on the following quantities: (1) the formation energy of the vacancy computed with respect to $\frac{1}{2}O_2$ $[E_f = E(TiO_{2-x}) - E(TiO_2) - E(\frac{x}{2}O_2)]$ for x =0.031; (2) the energy gap of the stoichiometric material, E_g; (3) and (4) the positions, ΔE_1 and ΔE_2 (see Fig. 2), of the

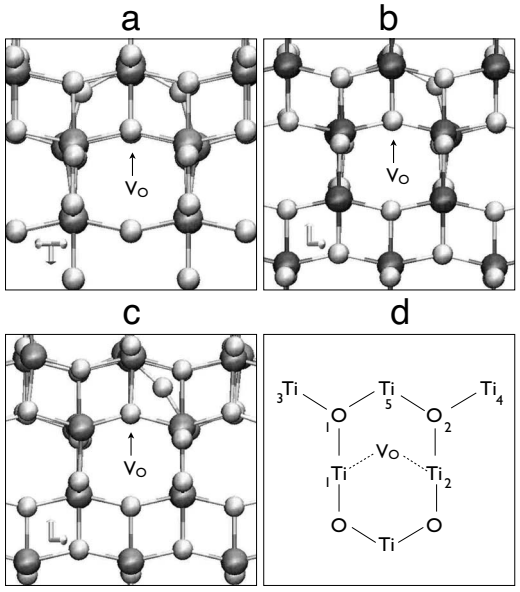

FIG. 1. Structural relaxation around an oxygen vacancy in anatase TiO_2. (a) PBE; (b) (U=3 eV); (c) B3LYP; (d) Schematic representation of the oxygen vacancy with atomic labels to identify selected interatomic distances in Table I. Ti atoms: black spheres, O atoms: white spheres.

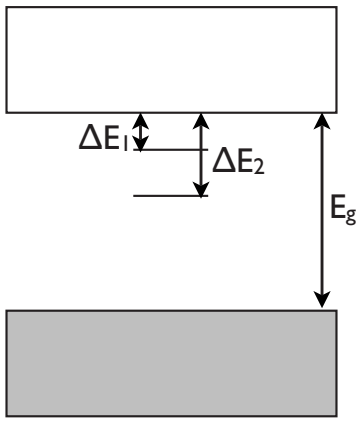

FIG. 2. Schematic representation of the band gap in bulk anatase TiO_2 and of the defect states associated to an oxygen vacancy.

TABLE II. Electronic properties of an O vacancy in bulk anatase TiO_2.

Method	U (eV)	E_f (eV)	E_g (eV)	ΔE_1 (eV)	ΔE_2 (eV)	Solution
PBE	···	4.30	2.60	0.21	0.30	2e delocalized
GGA+U	2	4.68	2.71	0.10	0.50	1e localized, 1e delocalized
GGA+U	3	4.55	2.79	0.57	0.95	2e localized
GGA+U	3	4.62	2.79	0.15	0.94	1e localized, 1e delocalized
GGA+U	4	4.24	2.87	1.07	1.46	2e localized
B3LYP	···	4.78	3.92	1.16	1.28	2e localized
B3LYP	···	4.84	3.92	0.59	1.35	1e localized, 1e delocalized
H&HLYP	···	4.24	6.82	5.03	5.08	2e localized

defect induced gap-states with respect to the bottom of the conduction band (CB) (each state corresponds to one electron which was formally associated to the removed O^{2-} ion and which is now redistributed over the crystal); (5) the spin density distribution.

Creating an O vacancy in bulk of anatase has a considerable energy cost, from 4.2 to 4.8 eV, see Table II, in line with previously reported estimates.[7] The formation energy differences among the various computational methods are moderate, of the order 10%, but these would be higher if one would consider as a reference an isolated O atom instead of the O_2 molecule.[7,76] This is because the dissociation energy of the O_2 molecule is well described by B3LYP (5.23 eV versus 5.18 eV in the experiment[77]) while it is overestimated by GGA (6.10 eV at the PBE level; results obtained at the molecular level with a 6-311+G^* basis set).

Differences are much more pronounced for the energy gaps. In Table II we report the gap computed at the Γ point for the stoichiometric oxide. Anatase TiO_2, however, has an indirect gap between $\sim X$ and Γ,[27] and for this reason the values reported are slightly overestimated compared to the real gap. The PBE band gap is 2.6 eV, i.e., about 0.6 eV smaller than the experimental one. The use of a GGA+U approach slightly increases this value: for $U=4$, this is relatively close to the experiment (2.87 eV versus 3.2 eV). B3LYP gives a direct gap of 3.92 eV, partly overestimated as already reported in the literature; it has been suggested that a 13% admixture of HF exchange is needed to obtain the correct gap[73] (for a detailed discussion of the performance of DFT functionals in reproducing the gap of rutile and anatase TiO_2 see also Ref. 75). H&HLYP gives a totally unrealistic gap of 6.82 eV; the material is no longer a semiconductor but becomes a wide gap insulator. The results of the H&HLYP calculations are reported for comparative purposes but clearly have little physical meaning given the large overestimate of the gap.

The value of the energy gap has profound consequences on the nature of the defect states associated to an O vacancy. The first case considered is that of the pure PBE functional. Here the solution is clear, unique, and unambiguous: the excess electrons associated to the missing oxygen are completely delocalized over the entire lattice, shared by all the Ti atoms of the cell, as shown by the spin density plot in Fig. 3(b). In the PDOS, Fig. 3(a), the bottom of the CB is near the Fermi level and is occupied. Due to the use of a limited number of k-points in the calculation of the PDOS, two states appear separated from the rest of the band: this is the reason of the finite values of ΔE_1 and ΔE_2 in Table II; however, the use of a larger number of k-points results in a merging of these states with the CB. The Ti ions around the vacancy do not contribute to the lower part of the CB, but their contribution is spread over a wide energy window. In summary, the two electrons are fully delocalized and have conduction band character. This result is not new as it is common to all GGA calculations of defective titania reported in the literature. Notice that the PBE calculations (and in general the GGA calculations) do not reproduce the feature of a peak well below the CB as observed in ultraviolet photoelectron spectroscopy (UPS) and electron energy loss spectroscopy (EELS) experiments.[43,44]

The picture is quite different when we use the GGA+U approach. Starting with $U=2$ eV, we found a state that is practically at the CB edge corresponding to a fully delocalized electron ($\Delta E_1=0.1$ eV) and a second state lower in energy $\Delta E_2=0.5$ eV, Figure 3(c). This second state corresponds to one electron in the 3d orbital of a Ti ion near the vacancy. The state is largely localized, as shown by the spin density plot, Fig. 3(d). Increasing the value of U, $U=3$ eV leads to two possible solutions. The first solution is slightly more stable and corresponds to two fully localized electrons. Both states are deep in the gap [$\Delta E_1=0.57$ eV, $\Delta E_2=0.95$ eV, Figure 3(e)] and the electrons occupy the 3d levels of two different Ti^{3+} ions, one of which is undercoordinated because it is near the vacancy, see Fig. 3(f). The second solution, less stable by 0.07 eV, corresponds to one electron localized ($\Delta E_2=0.94$ eV) and one delocalized ($\Delta E_1=0.15$ eV); both the LDOS and the spin density are similar to the $U=2$ eV case, Fig. 3(g) and 3(h). By further increasing the value of U, $U=4$ eV, the semilocalized solution is further destabilized and only the solution with both electrons localized is found, Table II. The two energy levels are 1.07 and 1.46 eV below the bottom of the CB, Fig. 3(i), and the spin density is even more concentrated on two specific Ti^{3+} ions, Fig. 3(l).

Next, we consider the results of the hybrid functionals. With B3LYP, the calculations converge to two solutions at very similar energy. The ground state corresponds to two electrons fully localized on two nonequivalent Ti ions, one of which is adjacent to the vacancy, see Fig. 3(n). The corresponding energy levels are at 1.16 and 1.28 eV below the

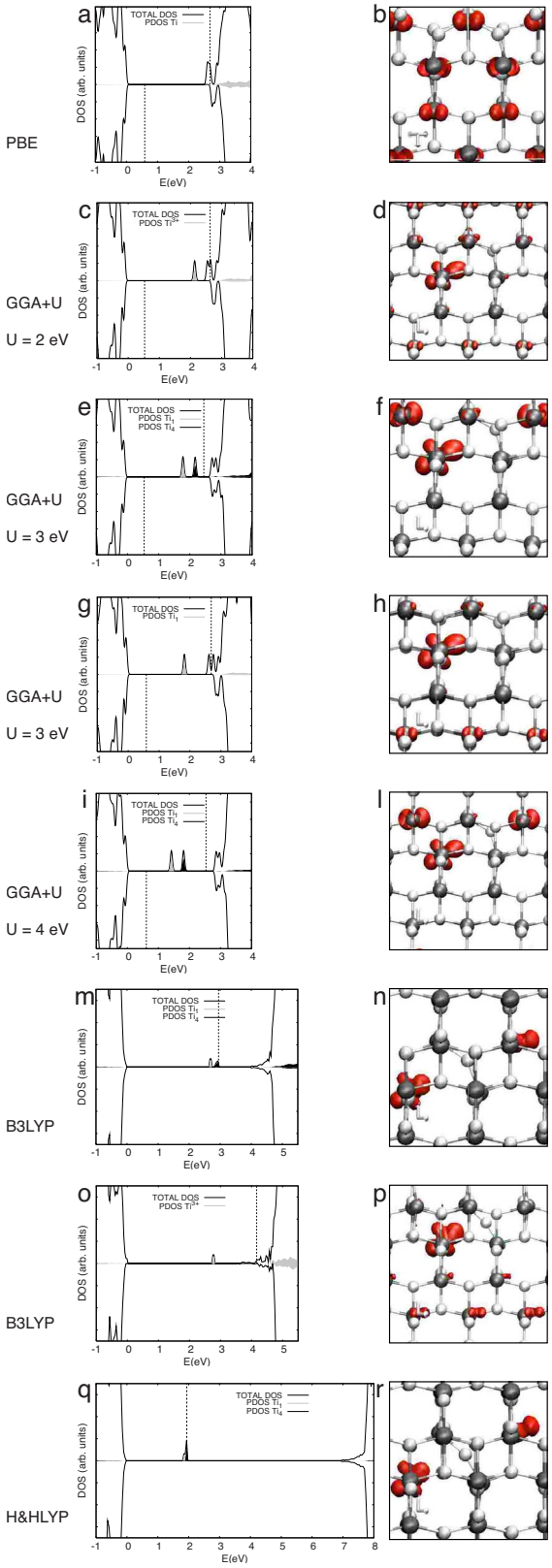

FIG. 3. (Color online) Total and partial density of states (PDOS projected on Ti, left) and spin distribution (right) for a oxygen vacancy in bulk anatase (triplet state). (a) and (b) PBE; (c) and (d) GGA+U (U=2 eV); (e) and (f) GGA+U (U=3 eV) 2e localized; (g) and (h) GGA+U (U=3 eV) 1e localized; (i) and (l) GGA+U (U=4 eV); (m) and (n) B3LYP 2e localized; (o) and (p) B3LYP 1e localized; (q) and (r) H&HLYP. The PDOS curves have been aligned by placing the top of the valence band at E=0. For CRYSTAL calculations the position of E_F for minority spin is not reported. Some of the atoms in the images are replicated and belong to the neighboring unit supercell. Ti atoms: black spheres, O atoms: white spheres.

CB, Fig. 3(m) and Table II. In the second solution, 0.06 eV higher in energy, one electron is localized in a state at 1.46 eV below the CB, Fig. 3(o), while the other electron is delocalized over a plane of Ti ions (not on the entire cell as in PBE), see Fig. 3(p). This latter state is 0.59 eV below the CB. The B3LYP results are thus surprisingly close to the solutions obtained at the GGA+U (U=3 eV) level. The strong asymmetry in the spin distribution is the reason for the strong asymmetry in the geometrical distortion around the defect. This polaronic distortion is more pronounced in B3LYP than in GGA+U, Table I.

The last case considered is that of the H&HLYP functional. As for the lowest B3LYP solution, the two electrons are fully localized on the two nonequivalent Ti ions nearest neighbors to the vacancy, Fig. 3(r), and the two impurity states lie deep in the gap, at about 5 eV below the bottom of the CB, Fig. 3(q). Clearly, this corresponds to a totally unrealistic description of defect states in TiO_2. Another state, slightly higher in energy (0.5 eV), is found where the two electrons are localized on both Ti atoms adjacent to the vacancy. The two Ti atoms being equivalent, the polaronic distortion around the defect is symmetrical.

To summarize this part, we have shown that the description of the electronic structure of an oxygen vacancy in bulk anatase TiO_2 is highly method dependent. Pure DFT functionals, such as PBE, give a completely delocalized solution and no states in the gap; the result of GGA+U calculations is strongly dependent on the value of U:[34] for U=2 eV or U=3 eV we have a solution with one electron localized and one electron delocalized, but for U=3 eV there is also a solution with both electrons localized which is slightly more stable. The localized electrons give rise to states in the gap at about 1 eV below the CB. A further increase in U (U=4 eV) gives only the solution where both electrons are localized and the states are deeper in the gap. The hybrid B3LYP functional is extremely similar to GGA+U for U=3 eV, with one solution where both electrons are fully localized and the second one with one localized and one more delocalized electron. This results in energy levels in the gap around 1 eV below CB. Hybrid methods with a larger weight of the HF exchange (e.g., H&HLYP) yield a gap that is too large and an unphysical localization and position of the states in the gap.

B. Hydrogen impurity in bulk anatase

Titania crystals can be reduced not only by creating oxygen vacancies (via thermal treatment, sputtering, etc.) but also by adding electron donors to the sample, alkali metals and hydrogen in particular. Alkali metals deposited on the surface of TiO_2 are known to act as electron donors with formation of an alkali metal cation adsorbed at the surface and an extra electron, which reduces Ti^{4+} to Ti^{3+}.[78] The same effect can be obtained by addition of atomic hydrogen, which splits into a proton bound to a lattice oxygen (forming an OH group) and an electron, which can be trapped at a Ti site, resulting in shallow traps.[3,79–81] Differently from the oxygen vacancy case, no clear experimental data seem to exist about

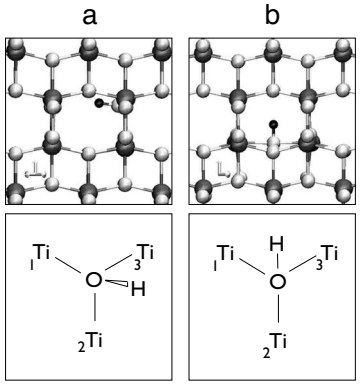

FIG. 4. Geometric structure of an H atom added to bulk anatase, PBE calculations. The scheme shows the orientation of the H atom with respect to a Ti–O–Ti plane. (a) Perpendicular; (b) co-planar. Ti atoms: black spheres, O atoms: white spheres.

the position of the gap states associated to an H impurity in anatase. The nature of this defect in bulk anatase is the topic of this paragraph.

In the unit cell of anatase TiO_2 there are two possible nonequivalent positions for a H atom added to a lattice oxygen. In one case the H atom is nearly perpendicular to the plane formed by $Ti_1-Ti_2-Ti_3$, Figure 4; in the other case the H atom is coplanar with these ions and is equidistant from the Ti_1 and Ti_3 atoms. An H atom has been added at short distance from oxygen (about 1 Å) in both positions, and the structure has been fully optimized at the PBE level, Fig. 4. Of the two situations, the "perpendicular" one, Fig. 4(a), is more stable by about 0.5 eV. In the following we concentrate on this configuration, as we assume that the localization/delocalization issue will be only moderately affected by the position of the OH group in the lattice.

The first property considered is the formation energy of the OH group, defined as $E_f = E(\text{H-TiO}_2) - E(\text{TiO}_2) - E(\frac{1}{2}\text{H}_2)$. A positive quantity indicates an endothermic process. Table III shows that all methods give a moderately endothermic reaction, with formation energies around 0.4–0.6 eV. An exception is provided by the H&HLYP calculation, which gives a nearly thermoneutral reaction due to the deep position in the gap of the corresponding impurity state (see below). Compared to the O vacancy case, the electronic structure here is simpler as we are dealing with only one extra electron to be accommodated in the unit cell.

The PBE solution is very similar to that obtained for the O vacancy case. The extra electron is completely delocalized over the entire cell, Fig. 5(b), and there are no states in the gap, Fig. 5(a) (the fact that there is one state at 0.07 eV below the CB, Table III, is, as we mentioned previously, related to the number of *k*-points used for the calculation of the LDOS). The four Ti–O equatorial distances around the Ti ion nearest neighbor of the OH group are rather short, 1.92–1.95 Å, Table III, and close to those of the undoped system, Table I. Thus, the physical picture is that H donates one electron to the CB of the material and this is fully delocalized.

In the GGA+U approach, with $U=2$ eV, we again obtain a delocalized solution, with a state at 0.08 eV below the CB, Fig. 5(c), and the spin distributed over all the Ti atoms of the cell, Fig. 5(d). By increasing the U value, $U=3$ eV and $U=4$ eV, we notice that the system can converge on two different solutions, one partly delocalized, and one almost completely localized. Let us consider $U=3$ eV, Table III. The localized solution shows that the unpaired electron is largely on the $3d$ levels of a Ti_{eq} ion nearest neighbor of the OH group, Fig. 5(f); the $Ti-O_{eq}$ distances increase to 1.97–2.01 Å as a consequence of the localization. The corresponding energy level is only 0.37 eV below the CB, Fig. 5(e). Interestingly, the delocalized solution is isoenergetic with the localized one; the spin is not distributed over all the Ti ions of the cell as in PBE but only on one particular plane of Ti ions, Fig. 5(h). No states in the gap are visible [$\Delta E_1 = 0.11$ eV, Figure 5(g)]; the Ti–O distances around the Ti ion near the OH group are short as in PBE. For $U=4$ the localized state is more stable by 0.13 eV than the delocalized one, the corresponding energy level is at 0.99 eV below the CB, Fig. 5(i), and there is a stronger polaronic distortion around the Ti ions carrying the spin, Fig. 5(l) (the Ti–O distances increase up to 2.04 Å, Table III). The other solution is only partly delocalized being the spin distributed over two Ti ions, Fig. 5(n); the corresponding electronic state is 0.42 eV below the CB, Table III and Fig. 5(m).

The results obtained with the hybrid B3LYP approach are very similar to those provided by the GGA+U, $U=3$ eV, method. Indeed, also with B3LYP we have been able to find two solutions of similar energy, Table III. One state corresponds to a fully localized solution, Fig. 5(p), which gives rise to a well defined state 0.94 eV below the CB, Fig. 5(o). The distortion around the Ti^{3+} ion is shown by the elongation of the equatorial Ti–O distances, Table III. The

TABLE III. Electronic properties and selected distances (in Å) of H-doped bulk anatase TiO_2.

Method	U (eV)	E_f (eV)	E_g (eV)	ΔE_1 (eV)	$d(\text{Ti}-\text{O}_{eq})$				$d(\text{Ti}-\text{O}_{ax})$		Solution
PBE	···	0.39	2.60	0.07	1.94	1.92	1.92	1.95	2.22	1.91	Delocalized
GGA+U	2	0.51	2.71	0.08	1.93	1.93	1.95	1.95	2.22	1.92	Delocalized
GGA+U	3	0.58	2.79	0.37	1.97	1.98	1.97	2.01	2.22	1.96	Localized
	3	0.58	2.79	0.11	1.93	1.93	1.94	1.94	2.22	1.92	Delocalized
GGA+U	4	0.47	2.87	0.99	2.00	2.02	1.96	2.04	2.23	2.04	Localized
	4	0.60	2.87	0.42	1.93	1.94	1.93	1.93	2.22	1.92	Delocalized
B3LYP	···	0.74	3.92	0.94	2.01	2.02	1.98	2.02	2.23	2.03	Localized
	···	0.56	3.92	0.55	1.94	1.93	1.96	1.96	2.24	1.93	Delocalized
H&HLYP	···	−0.09	6.82	4.84	2.03	2.04	2.02	2.02	2.22	2.03	Localized

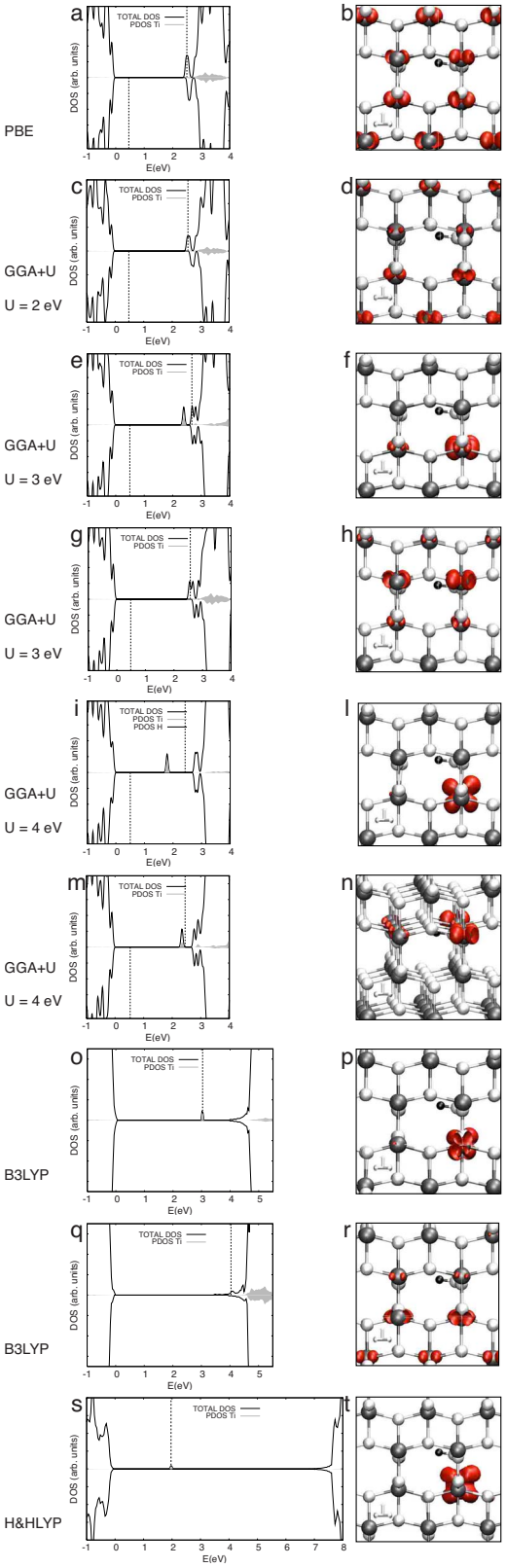

FIG. 5. (Color online) Total and partial density of states (PDOS projected on Ti and H, left) and spin distribution (right) for a hydrogen impurity in bulk anatase. (a) and (b) PBE; (c) and (d) GGA+U (U=2 eV); (e) and (f) GGA+U (U=3 eV) localized; (g) and (h) GGA+U (U=3 eV) delocalized; (i) and (l) GGA+U (U=4 eV) localized; (m) and (n) GGA+U (U=4 eV) delocalized; (o) and (p) B3LYP localized; (q) and (r) B3LYP delocalized; (s) and (t) H&HLYP. The PDOS curves have been aligned by placing the top of the valence band at E=0. For Crystal calculations the position of E_F for minority spin is not reported. Ti atoms: black spheres, O atoms: white spheres.

other solution, 0.18 eV lower in energy (ground state), corresponds to a state 0.55 eV below the CB, Fig. 5(q), which is delocalized over only part of the Ti atoms of the cell, Fig. 5(r). The last case considered is that of the H&HLYP hybrid functional. Here, as for the O vacancy, only one strongly localized solution is found, Fig. 5(t), with a state deep in the gap, 4.8 eV below the CB, Fig. 5(s).

IV. DISCUSSION AND CONCLUSIONS

As mentioned in Sec. I, titanium dioxide is a technologically very important material in various fields (photochemistry, optical properties, pigment industry, nanoparticles, biocompatible material, hybrid solar cells, etc.). Consequently, also the number of theoretical studies on TiO_2 is extremely large. Anatase is the most common form of TiO_2 and is the one that is found in most applications. TiO_2 samples are never perfectly stoichiometric, and are usually in reduced form, an aspect which is very important to determine the final properties of the material. For all these reasons, an accurate theoretical description of the electronic structure of a common intrinsic defect like a bulk O vacancy would be extremely useful. Here we have considered this defect center and, for comparison, we also considered a hydrogen impurity, which is an electron donor like the O vacancy. The results of the present work show, however, that the present theoretical understanding is far from satisfactory. The nature of the defect states in reduced TiO_2 is strongly dependent on the method used. This is not a new conclusion. What emerges from the present study, however, is that there is a continuous variation in the computed properties as a function of the parameters that are introduced to correct the deficiencies of the pure DFT approach.

Because of the inaccurate description of the self-interaction and of the too low band gap, in pure DFT (here we considered the PBE functional) the states associated to the defect (either an O vacancy or an OH group) are completely delocalized and the corresponding LDOS does not show any state in the gap, at variance with the experimental evidence. A way to correct the deficiency of pure DFT is to use the GGA+U approach. The results reported above clearly show that there are two possible solutions for the problem: in one case an electron is localized on a single Ti ion, while in the other case the electron is delocalized over several Ti ions. Depending on the degree of localization, the corresponding energy level is deep in the gap (localized solution) or close to the CB (delocalized solution). For the O vacancy, we found solutions where one electron is fully localized and one partly delocalized, with two distinct energy levels in the gap. Notice that there is no sign of such a splitting of levels in the experiment: given the instrumental resolution and the spectral broadening, the splitting is at most of 0.1–0.2 eV. The situation changes continuously by tuning the U value and there does not seem to exist any simple way to determine the "right" U value. The major improvement of GGA+U compared to pure DFT is that the energy gap of the material is better described, and the impurity state in the gap is obtained. When both electrons are localized on two nonequivalent Ti ions the defect states are

separated by 0.3–0.4 eV, and located at about 1 eV below the conduction band, in broad agreement with the experiment.

Hybrid functionals show the same characteristics of the GGA+U approach. Here what changes is the amount of HF exchange introduced in the Hamiltonian. In the popular B3LYP approach the amount of the HF exchange (20%) has been derived by fitting thermochemical data on a series of simple molecules.[65] There is no fundamental reason why this contribution should be the right one to describe defects in insulating or semiconducting oxides. For the specific problem of reduced anatase TiO_2, B3LYP behaves very similar as a GGA+U approach with $U=3$. Also in this case the presence of an impurity state in the gap is qualitatively reproduced, while the computed gap is larger than the experimental one. As for the GGA+U, in B3LYP a semi-localized solution corresponds to two well separated impurity states, at variance with the observations; however, the lowest energy corresponds to two fully localized electrons with the associated gap states at about 1.2 eV below the conduction band and separated by 0.1 eV only. If we consider that the gap in B3LYP is overestimated by about 20%, this would correspond to a single state at about 1 eV below the conduction band in the real system, in quite good agreement with the observation. By increasing the amount of HF exchange (here we considered the case of the H&HLYP functional with 50% of HF exchange) the results become unphysical and have no value for the present discussion. Notice, however, that for other systems (e.g., NiO) (Refs. 20 and 82) the use of hybrid methods with a larger portion of HF exchange provides better results than B3LYP and that in the case of an Al-impurity in SiO_2 only the HF method is able to yield a localized hole, in agreement with experiment.[11]

Our results show that the theoretical description of reduced titania, and in general of other reducible transition metal oxides like ZrO_2 or CeO_2, is not straightforward, should be performed by comparing various computational methods, and additionally needs careful validation by comparison with experimental results. Also in this respect, however, the situation is far from simple, as spectroscopic fingerprints of the nature of defects in reduced titania are not unambiguous and often depend on a number of external conditions (sample preparation, temperature at which the experiment is done, surface area of the sample, level of reduction, sensitivity to surface or to bulk defects of the experimental technique, etc.). A great contribution could come from electron paramagnetic resonance (EPR), as the Ti^{3+} ions have a clear EPR signal. Unfortunately, Ti has no nuclear spin so that hyperfine interactions are not available and in order to measure superhyperfine interactions with the O ions one should prepare ^{17}O enriched samples, a very costly procedure. In the absence of these experiments, a direct validation of theory is not currently available and we honestly admit that at the moment theory is unable to provide firm conclusions about the nature of defect states in reduced titania. Unambiguous experimental information on well defined systems of reduced complexity or calculations performed at a higher level of theory can provide the key to solve this issue.

ACKNOWLEDGMENTS

This work has been supported by the Italian MIUR through a PRIN 2005 project and the COST Action D41 "Inorganic oxide surfaces and interfaces." One of us (E.F.) thanks the financial support during his stay at the Department of Chemistry of Princeton University. We thank Dr. X.-Q. Gong for fruitful discussions.

[1] J. L. Gavartin, P. V. Sushko, and A. L. Shluger, Phys. Rev. B **67**, 035108 (2003).
[2] J. Sauer and J. Döbler, Dalton Trans. **19**, 3116 (2004).
[3] C. Di Valentin, G. Pacchioni, and A. Selloni, Phys. Rev. Lett. **97**, 166803 (2006).
[4] S. Sicolo, G. Palma, C. Di Valentin, and G. Pacchioni, Phys. Rev. B **76**, 075121 (2007).
[5] A. M. Stoneham, *Theory of Defects in Solids* (Oxford University Press, Oxford, 1975).
[6] R. J. D. Tilley, *Principles and Applications of Chemical Defects* (Stanley Thornes, Cheltenham, 1998).
[7] M. V. Ganduglia-Pirovano, A. Hofman, and J. Sauer, Surf. Sci. Rep. **62**, 219 (2007).
[8] J. H. E. Griffiths, J. Owen, and I. M. Ward, Nature (London) **173**, 439 (1954).
[9] M. C. M. O'Brien, Proc. R. Soc. London, Ser. A **231**, 404 (1955).
[10] R. H. D. Nuttall and J. A. Weil, Can. J. Phys. **59**, 1696 (1981)..
[11] G. Pacchioni, F. Frigoli, D. Ricci, and J. A. Weil, Phys. Rev. B **63**, 054102 (2000).
[12] J. Laegsgaard and K. Stokbro, Phys. Rev. Lett. **86**, 2834 (2001).
[13] J. To, A. A. Sokol, S. A. French, N. Kaltsoyannis, and C. R. A. Catlow, J. Chem. Phys. **122**, 144704 (2005).
[14] X. Solans-Monfort, V. Branchadell, M. Sodupe, M. Sierka, and J. Sauer, J. Chem. Phys. **121**, 6034 (2004).
[15] M. Nolan and G. W. Watson, J. Chem. Phys. **125**, 144701 (2006).
[16] M. Magagnini, P. Giannozzi, and A. Dal Corso, Phys. Rev. B **61**, 2621 (2000).
[17] J. Laegsgaard and K. Stokbro, Phys. Rev. B **61**, 12590 (2000).
[18] R. G. Parr and W. Yang, *Density Functional Theory of Atoms and Molecules* (Oxford Science, Oxford, 1989).
[19] W. Koch and M. C. Holthausen, *A Chemist Guide to Density Functional Theory* (Wiley, Weinheim, 2002).
[20] I. de P. R. Moreira, F. Illas, and R. L. Martin, Phys. Rev. B **65**, 155102 (2002).
[21] M. Sodupe, J. Bertran, L. Rodriguez-Santiago, and E. J. Baerends, J. Phys. Chem. A **103**, 166 (1999).
[22] L. Hedin, Phys. Rev. **139**, A796 (1965).
[23] V. I. Anisimov, J. Zaanen, and O. K. Andersen, Phys. Rev. B **44**, 943 (1991).
[24] M. Cococcioni and S. De Gironcoli, Phys. Rev. B **71**, 035105 (2005).
[25] V. E. Henrich and R. L. Kurtz, Phys. Rev. B **23**, 6280 (1981).
[26] H. Tang, F. Lévy, H. Berger, and P. E. Schmid, Phys. Rev. B **52**, 7771 (1995).
[27] H. Tang, H. Berger, P. E. Schmid, and F. Lévy, Solid State Commun. **87**, 847 (1993).
[28] R. Asahi, Y. Taga, W. Mannstadt, and A. J. Freeman, Phys. Rev. B **61**, 7459 (2000).
[29] J. Muscat, V. Swamy, and N. M. Harrison, Phys. Rev. B **65**, 224112 (2002).
[30] J. C. Woicik, E. J. Nelson, L. Kronik, M. Jain, J. R. Chelikowsky, D. Heskett, L. E. Berman, and G. S. Herman, Phys. Rev. Lett. **89**, 077401 (2002).
[31] X. Chen and S. S. Mao, Chem. Rev. (Washington, D.C.) **107**, 2891 (2007).
[32] T. L. Thompson and J. T. Yates, Chem. Rev. (Washington, D.C.) **106**, 4428 (2006).
[33] U. Diebold, Surf. Sci. Rep. **48**, 53 (2003).
[34] B. J. Morgan and G. W. Watson, Surf. Sci. **601**, 5034 (2007); C. J. Calzado, N. C. Hernandez, and J. F. Sanz, Phys. Rev. B **77**, 045118 (2008).
[35] A. Bouzoubaa, A. Markovits, M. Calatayud, and C. Minot, Surf. Sci. **583**, 107 (2005).
[36] S. Na-Phattalung, M. F. Smith, K. Kim, M.-H. Du, S.-H. Wei, S. B. Zhang, and S. Limpijumnong, Phys. Rev. B **73**, 125205 (2006).

[37] X. Zuo, S.-D. Yoon, A. Yang, C. Vittoria, and V. G. Harris, J. Appl. Phys. **103**, 07B911 (2008).
[38] T. Bredow and G. Pacchioni, Chem. Phys. Lett. **355**, 417 (2002).
[39] C. Di Valentin, J. Chem. Phys. **127**, 154705 (2007).
[40] V. E. Henrich, G. Dresselhaus, and H. J. Geiger, Phys. Rev. Lett. **36**, 1335 (1976).
[41] G. Lu, A. Linsebigler, and J. T. Yates, J. Phys. Chem. **98**, 11733 (1994).
[42] V. M. Khomenko, K. Langer, H. Rager, and A. Fett, Phys. Chem. Miner. **25**, 338 (1998).
[43] M. A. Henderson W. S. Epling, C. H. F. Peden, and C. L. Perkins, J. Phys. Chem. B **107**, 534 (2003).
[44] R. L. Kurtz, R. Stock-Bauer, and T. E. Madey, Surf. Sci. **218**, 178 (1989).
[45] R. Doreswamy Iyengar, M. Codell, J. S. Karra, and J. Turkevich, J. Am. Chem. Soc. **88**, 5055 (1966).
[46] E. Serwicka, M. W. Schlierkamp, and R. N. Schindler, Z. Naturforsch. **36A**, 226 (1981)..
[47] D. C. Hurum, A. G. Agrios, K. A. Gray, T. Rajh, and M. C. Thurnauer, J. Phys. Chem. B **107**, 4545 (2003).
[48] T. Berger, M. Sterrer, O. Diwald, E. Knözinger, D. Panayotov, T. L. Thompson, and J. T. Yates, J. Phys. Chem. B **109**, 6061 (2005).
[49] D. C. Hurum, A. G. Agrios, K. A. Gray, T. Rajh, and M. C. Thurnauer, J. Phys. Chem. B **107**, 4545 (2003).
[50] J. Nerlov, S. V. Christensen, S. Wichel, E. H. Pedersen, and P. J. Møller, Surf. Sci. **371**, 321 (1997).
[51] M. Li, W. Hebenstreit, U. Diebold, A. M. Tryshkin, M. K. Bowman, G. G. Dunhan, and M. Henderson, J. Phys. Chem. B **104**, 4944 (2000).
[52] M. Ménétrey, A. Markovits, and C. Minot, Surf. Sci. **524**, 49 (2003).
[53] M. D. Rasmussen, L. M. Molina, and B. Hammer, J. Chem. Phys. **120**, 988 (2004).
[54] X. Y. Wu, A. Selloni, and S. K. Nayak, J. Chem. Phys. **120**, 4512 (2004).
[55] M. Calatayud, P. Mori-Sanchez, A. Beltran, A. Martin Pendas, E. Francisco, J. Andrei, and J. M. Recio, Phys. Rev. B **64**, 184113 (2001).
[56] A. M. Czoska, S. Livraghi, M. Chiesa, E. Giamello, S. Agnoli, G. Granozzi, E. Finazzi, C. Di Valentin, and G. Pacchioni, J. Phys. Chem. C **112**, 8951 (2008)..
[57] M. A. Henderson, Surf. Sci. **419**, 174 (1999).
[58] H. Onishi and Y. Iwasawa, Phys. Rev. Lett. **76**, 791 (1996).
[59] R. A. Bennett, P. Stone, N. J. Price, and M. Bowker, Phys. Rev. Lett. **82**, 3831 (1999).
[60] M. Valden, X. Lai, and D. W. Goodman, Science **281**, 1647 (1998).
[61] S. Wendt, P. T. Sprunger, E. Lira, G. K. H. Madsen, Z. Li, J. O. Hansen, J. Matthiasen, A. Blekinge-Rasmussen, E. Laegsgaard, B. Hammer, and F. Besenbacher, Science **320**, 1755 (2008).
[62] P. Perdew, K. Burke, and M. Ernzerhof, Phys. Rev. Lett. **77**, 3865 (1996).
[63] A. I. Liechtenstein, V. I. Anisimov, and J. Zaanen, Phys. Rev. B **52**, R5467 (1995).
[64] S. L. Dudarev, G. A. Botton, S. Y. Savrasov, C. J. Humphreys, and A. P. Sutton, Phys. Rev. B **57**, 1505 (1998).
[65] A. D. Becke, J. Chem. Phys. **98**, 5648 (1993).
[66] C. Lee, W. Yang, and R. G. Parr, Phys. Rev. B **37**, 785 (1988).
[67] S. Baroni, S. De Gironcoli, A. Dal Corso, and P. Giannozzi, (http://www.pwscf.org).
[68] V. R. Saunders, R. Dovesi, C. Roetti, R. Orlando, C. M. Zicovich-Wilson, N. M. Harrison, K. Doll, B. Civalleri, I. J. Bush, Ph. D'Arco, and M. Llunell, *CRYSTAL03 User's Manual* (University of Torino, Torino, 2003).
[69] C. M. Zicovich-Wilson and R. Dovesi, J. Phys. Chem. B **102**, 1411 (1998).
[70] E. Ruiz, M. Llunlell, and P. Alemany, J. Solid State Chem. **176**, 400 (2003).
[71] A. D. Becke, J. Chem. Phys. **98**, 1372 (1993).
[72] M. Lazzeri, A. Vittadini, and A. Selloni, Phys. Rev. B **63**, 155409 (2001).
[73] Y. Zhang, W. Lin, Y. Li, K. N. Ding, and J. Q. Li, J. Phys. Chem. B **109**, 19270 (2005).
[74] J. K. Burdett, T. Hughbanks, G. J. Miller, J. W. Richardson, and J. V. Smith, J. Am. Chem. Soc. **109**, 3639 (1987).
[75] F. Labat, P. Baranek, C. Domain, C. Minot, and C. Adamo, J. Chem. Phys. **126**, 154703 (2007).
[76] G. Pacchioni, J. Chem. Phys. **128**, 182505 (2008).
[77] G. Herzberg, *Molecular Spectra and Molecular Structure. I. Spectra of Diatomic Molecules* (Robert E. Krieger, Malabar, FL, 1989).
[78] T. Bredow, E. Aprà, M. Catti, and G. Pacchioni, Surf. Sci. **418**, 150 (1998).
[79] D. A. Panayotov and J. T. Yates, Chem. Phys. Lett. **436**, 204 (2007).
[80] P. W. Peacock and J. Robertson, Appl. Phys. Lett. **83**, 2025 (2003).
[81] M. V. Koudriachova, S. W. De Leeuw, and N. M. Harrison, Phys. Rev. **70**, 165421 (2004)..
[82] T. Bredow and A. R. Gerson, Phys. Rev. B **61**, 5194 (2000).